

Electronic Supporting Information

Exploration of the mechanical behavior of rigid Metal Organic Frameworks UiO-66(Zr) and MIL-125(Ti) and their NH₂ functionalized versions

Pascal. G. Yot,^{*a} Ke Yang,^a Florence Ragon,^b Vladimir Dmitriev,^c Thomas Devic,^b
Patricia Horcajada,^b Christian Serre,^b Guillaume Maurin^a

- a. Institut Charles Gerhardt Montpellier (UMR 5253), Université de Montpellier,
CC 15005, Place Eugène Bataillon, F-34095 Montpellier cedex 05, France.
e-mail: pascal.yot@umontpellier.fr; Tel: +33 4 67 14 32 94; Fax: +33 4 67 14
42 90.
- b. Institut Lavoisier Versailles (UMR 8180), Université de Versailles St-Quentin,
45, avenue des Etats-Unis, F-78035 Versailles cedex, France.
- c. Swiss Norwegian Beamlines, European Synchrotron Radiation Facility, 3800
Grenoble, France.

1. Synthesis and thermal characterisations

1.1. UiO-66(Zr) Synthesis:

UiO-66(Zr) sample was synthesised using the following procedure inspired from [1]: a mixture of 1.66 g of terephthalic acid (10 mmol), 1.16 g of zirconium(IV) chloride (5 mmol) and 0.8 mL of a 37% aqueous solution of hydrochloric acid (10 mmol) in 30 mL of N, N-dimethylformamide (DMF) was placed in a 125 mL Parr autoclave and heated at 220°C for 17 hours. The resulting white solid was recovered by filtration, washed with DMF, methanol and finally dried at 180°C under primary vacuum.

1.2. UiO-66(Zr)_NH₂ Synthesis:

The synthesis of UiO-66(Zr)_NH₂ material was performed under solvothermal conditions following a modified procedure of the previously reported protocol [2]. Typically, 1 mmol of zirconium (IV) chloride (ZrCl₄) and 1 mmol of the aminoterephthalic acid were dispersed in 3 mL of dimethylformamide (DMF), placed in a Teflon-lined autoclave and heated at 100°C for 24 h. The resulting solid was recovered by filtration and washed with deionized water and acetone. After filtration, the activation was carried out by suspending 200 mg of the solid in 100 mL of DMF under stirring for 12 h. Then, the DMF-washed solid was suspended in 100 mL of MeOH under stirring for 12 h, recovering the activated solid by filtration.

The purity and composition of the solid was assessed by powder XRD, IR spectroscopy and TG analyses.

1.3. Thermo Gravimetric Analysis:

By considering the formula Zr₆O₆L_n at 300°C and following the method proposed by Shearer *et al.* [3], we evaluated the concentration of missing linkers in UiO-66(Zr)s by TGA :

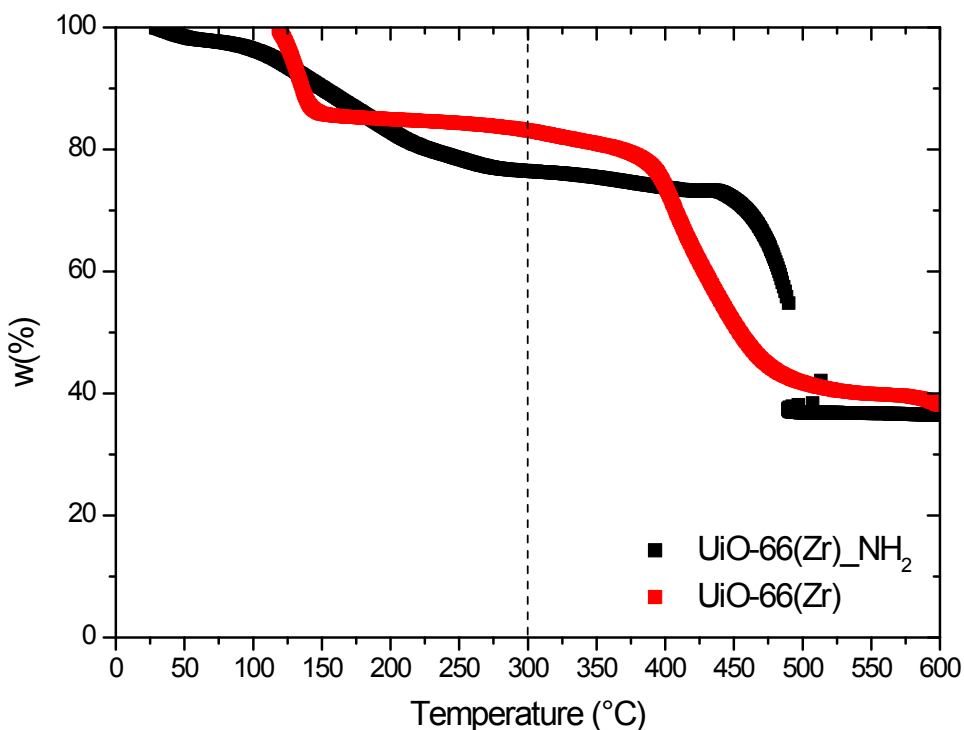


Figure S1. Thermal Gravimetric Analysis curve obtained for $\text{UiO-66}(\text{Zr})$ solid and its amino version under oxygen atmosphere.

Table 1. Weight losses at 300°C and 600°C , number of organic linkers and degree of missing linkers in both $\text{UiO-66}(\text{Zr})$ s.

	Weight loss at 300°C	Weight loss at 300°C	Number linkers	Degree of missing linkers
$\text{UiO-66}(\text{Zr})$	76.5	36.5	5.5	8.3 %
$\text{UiO-66}(\text{Zr})_{\text{NH}_2}$	83.1	38.1	5.4	10 %

Weight losses obtained for $\text{UiO-66}(\text{Zr})$ and $\text{UiO-66}(\text{Zr})_{\text{NH}_2}$ reported in Table S1 allow the determination of the number of organic linker for both solids by considering the chemical equation for decomposition of (dehydroxylated) UiO-66 [3]:



The number of organic linker are closed to 5.5 for both solids close to the theoretical value of 6 obtained from the chemical formula, thus leading to a concentration of missing linker ~9%.

2. Synchrotron X-ray powder diffraction

Diffraction patterns were collected using MAR345 image plate detector, a monochromatic beam with the wavelength of 0.694120 Å and a time of exposition of 3 minutes. Pressures were generated a DAC with flat culets of diameter 600 µm. The powder was loaded into a hole of 250 µm in diameter drilled in a stainless steel gasket preindented to 60-80 µm thickness; the beam was slit collimated to 100x100 µm². Pressures were measured from the shift of the ruby R1 fluorescence line [4]. The sample to-detector distance (350 mm) and parameters of the detector were calibrated using NIST standard LaB₆. Two-dimensional diffraction images were integrated using FIT2D software [5]. Quasi-hydrostatic conditions were provide by Silicone oil (AP100, Fluka). All diffraction measurements were performed increasing and decreasing the pressure in the range 10⁻⁷-3 GPa. The unit-cell parameters were determined by indexing the X-ray powder diffraction patterns, using DICVOL6 [6] followed by a Le Bail fit using Jana 2006 software [7].

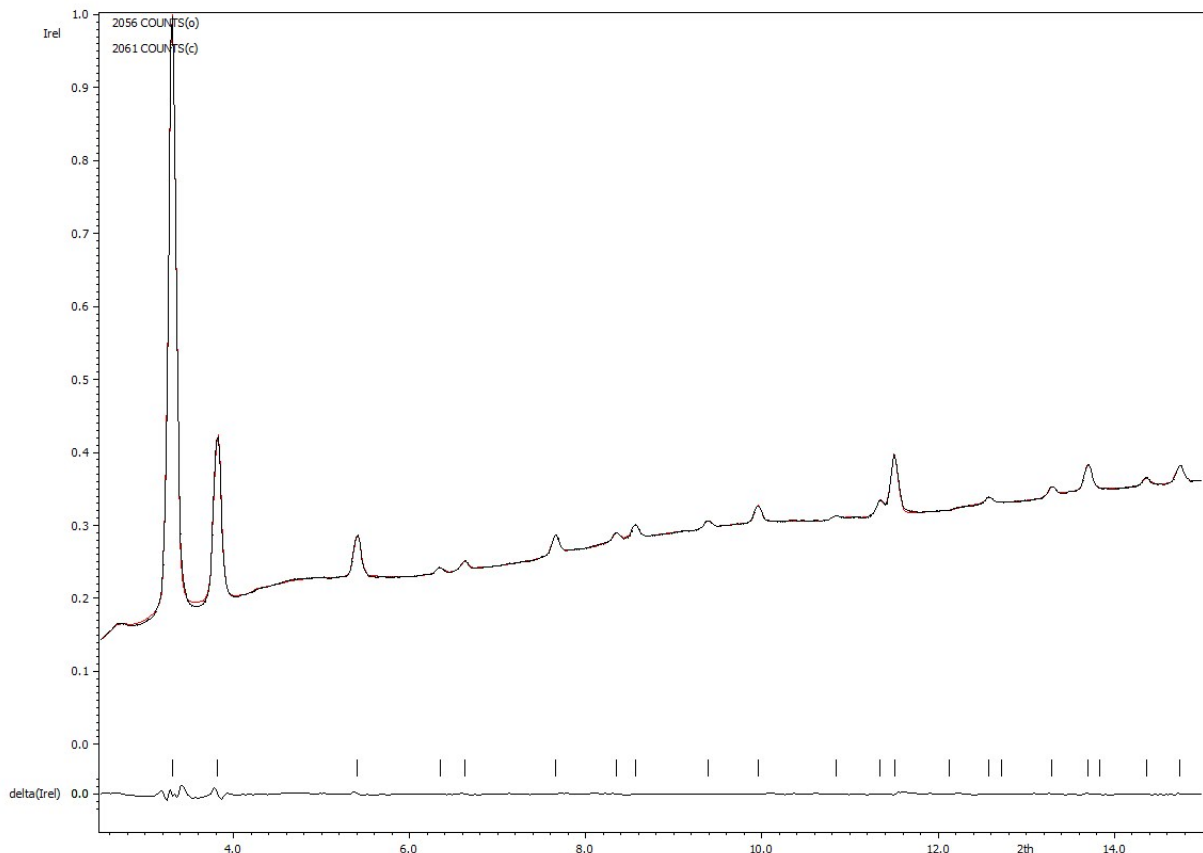


Figure S2. Structure-independent refinement of the unit-cell of the diffraction pattern obtained for the UiO-66(Zr), space group F $\bar{4}3m$: $a=20.753(1)$ Å, $V=8938.2(1)$ Å³ (R_p : 0.31, R_{wp} : 0.61) at atmospheric pressure (first step of the experiment).

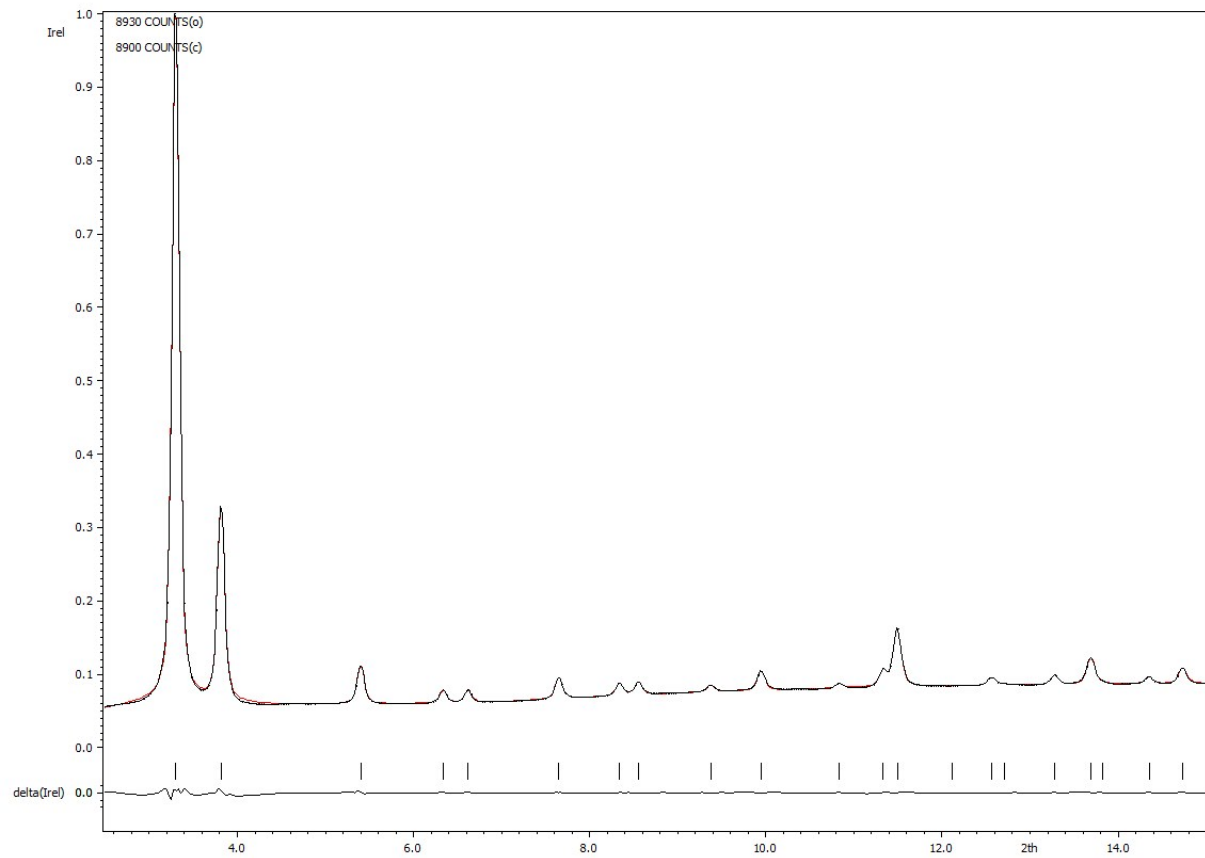


Figure S3. Structure-independent refinement of the unit-cell of the diffraction pattern obtained for the $\text{UiO-66}(\text{Zr})\text{-NH}_2$, space group $\text{F}\bar{4}3\text{m}$: $a=20.770(6)$ Å, $V=9026.9(3)$ Å³ (R_p : 0.73, R_{wp} : 0.88) at atmospheric pressure (first step of the experiment).

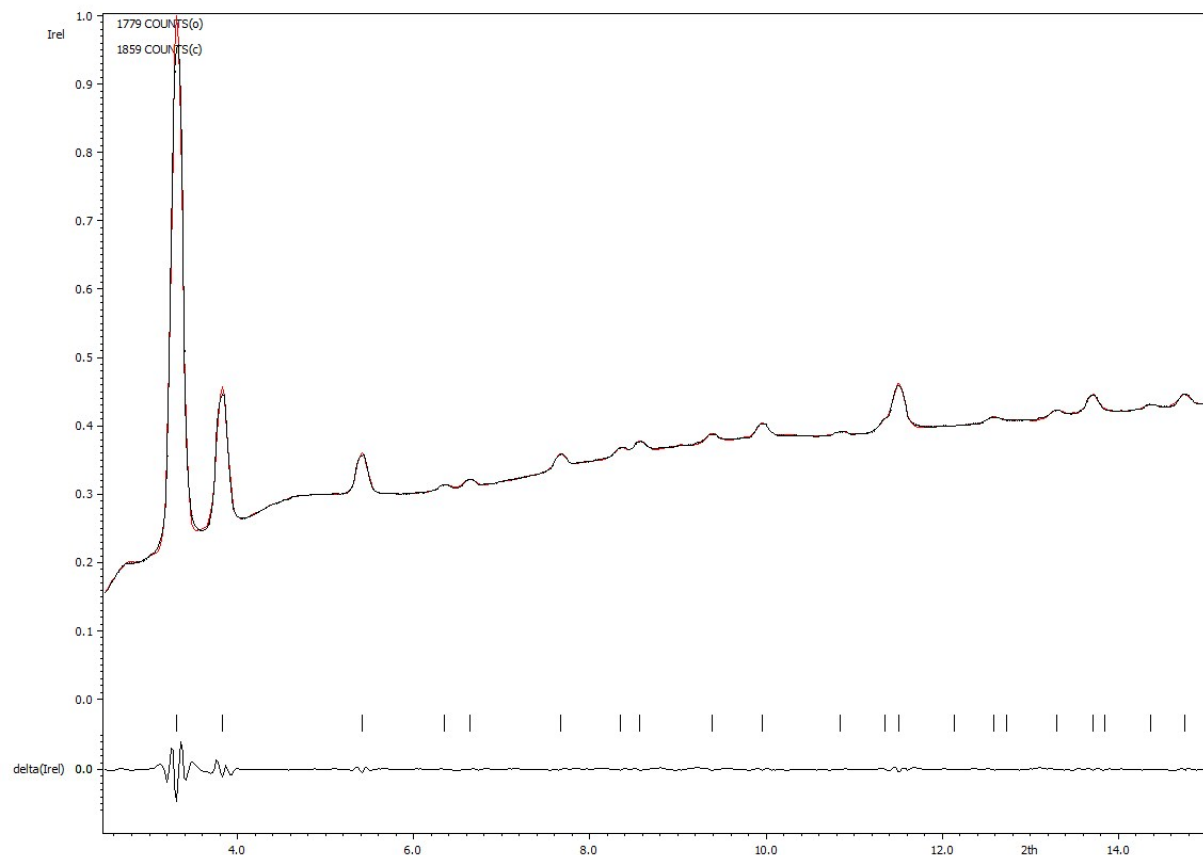


Figure S4. Structure-independent refinement of the unit-cell of the diffraction pattern obtained for the $\text{UiO-66}(\text{Zr})$, space group $\bar{\text{F}}\bar{4}\bar{3}\text{m}$: $a=20.762(3)\text{\AA}$, $V=8982.4(1)\text{\AA}^3$ ($R_p: 0.32$, $R_{wp}: 0.77$) at atmospheric pressure after releasing the pressure (last step of the experiment).

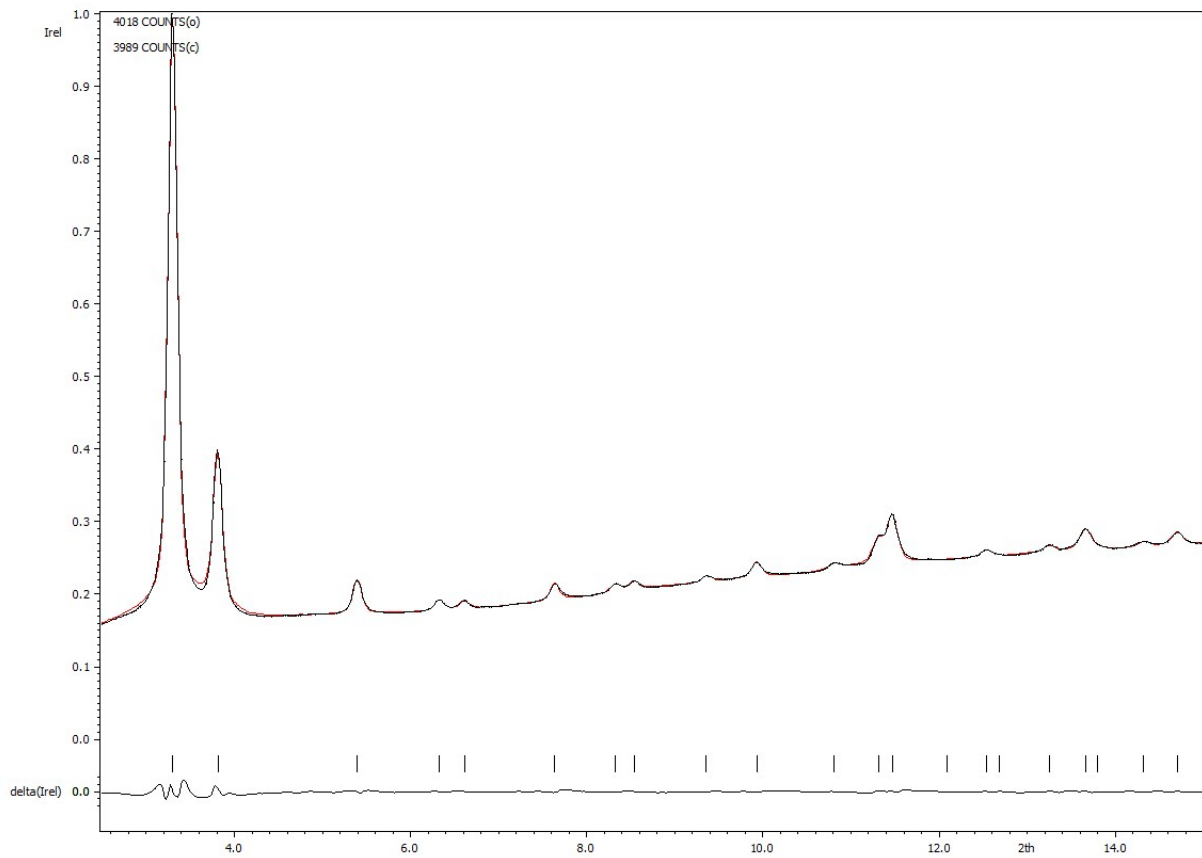


Figure S5. Structure-independent refinement of the unit-cell of the diffraction pattern obtained for the $\text{UiO-66}(\text{Zr})\text{-NH}_2$, space group $\text{F}\bar{4}3\text{m}$: $a=20.321(2)\text{\AA}$, $V=9034.2(1)\text{\AA}^3$ (R_p : 0.55, R_{wp} : 0.64) at atmospheric pressure after releasing the pressure (last step of the experiment).

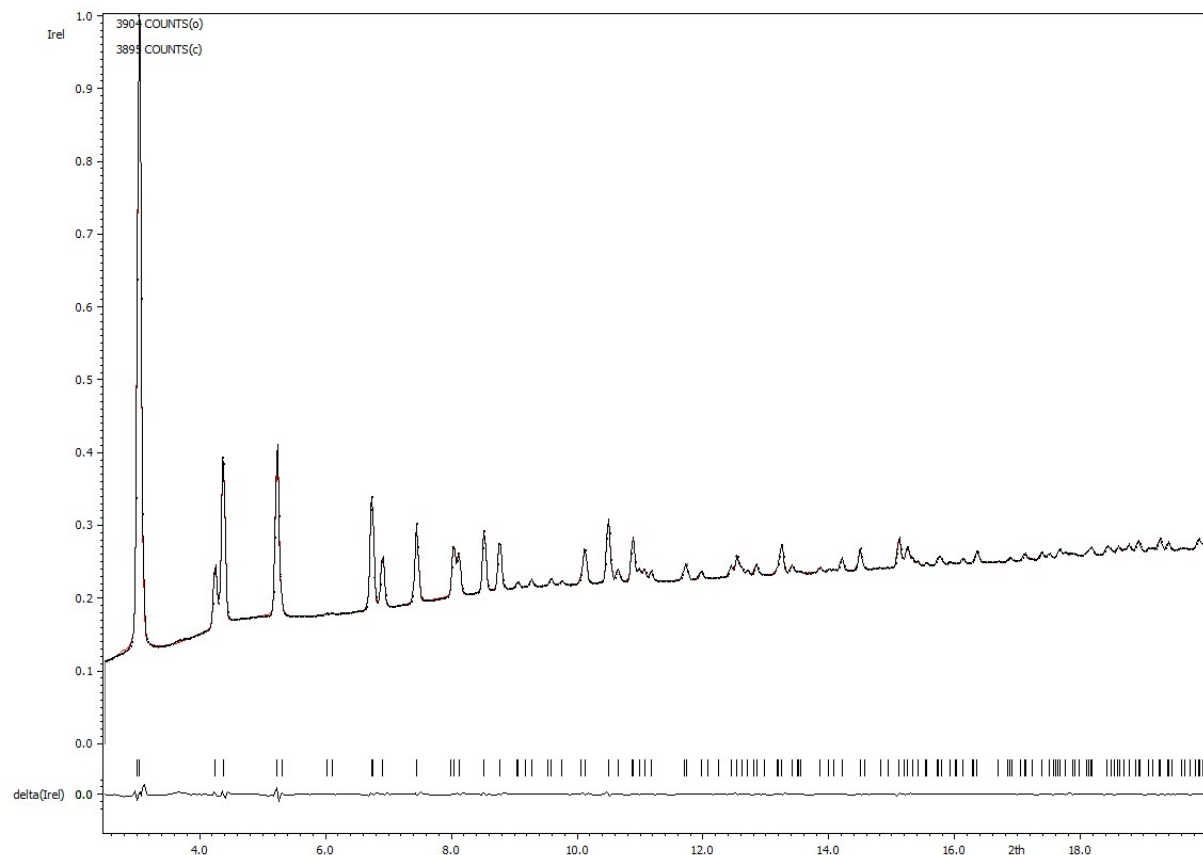


Figure S6. Structure-independent refinement of the unit-cell of the diffraction pattern obtained for the MIL-125(Ti), space group I4/mmm: $a=18.6466(3)$ Å, $c=18.1253(5)$ Å, $V=6302.8(3)$ Å 3 (R_p : 0.23, R_{wp} : 0.28) (first step of the experiment).

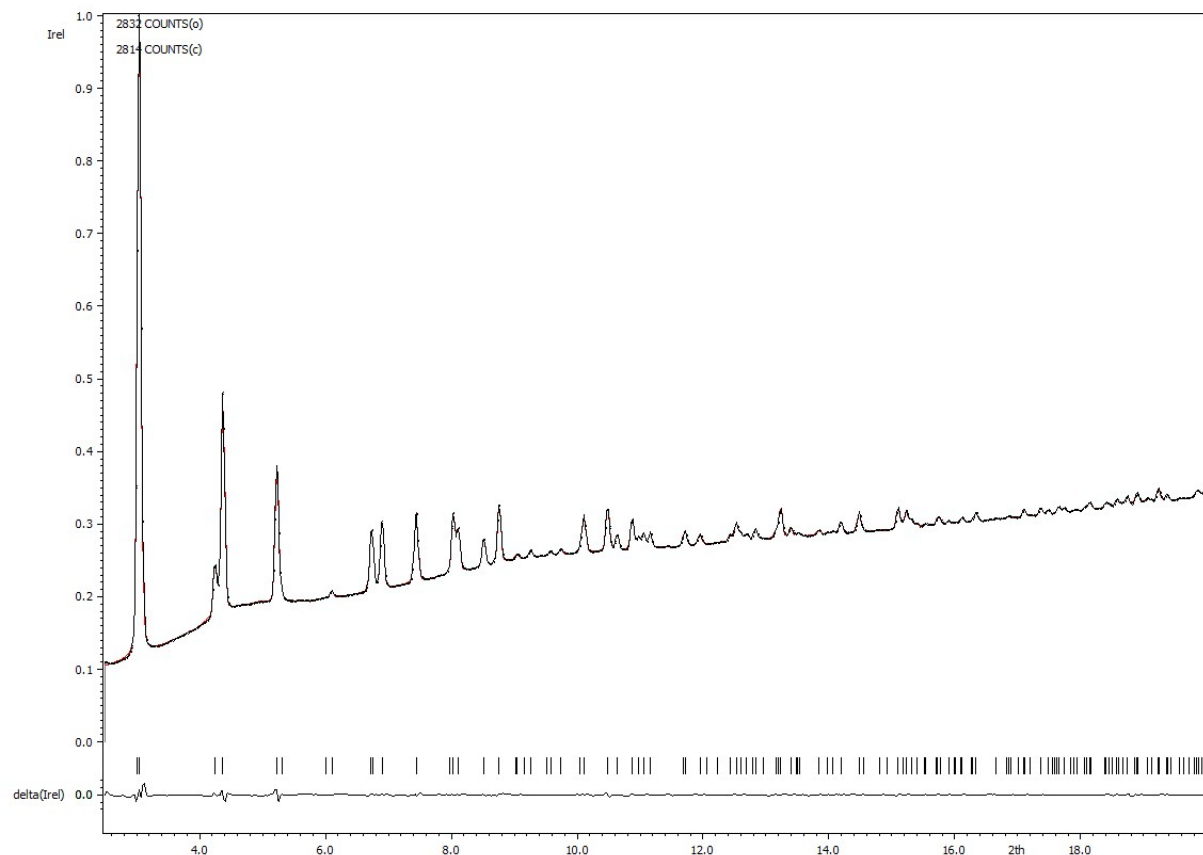


Figure S7. Structure-independent refinement of the unit-cell of the diffraction pattern obtained for the MIL-125(Ti)_nNH₂, space group I4/mmm: $a=18.6680(3)$ Å, $c=18.1504(5)$ Å, $V=6325.6(4)$ Å³ (R_p : 0.21, R_{wp} : 0.26) (first step of the experiment).

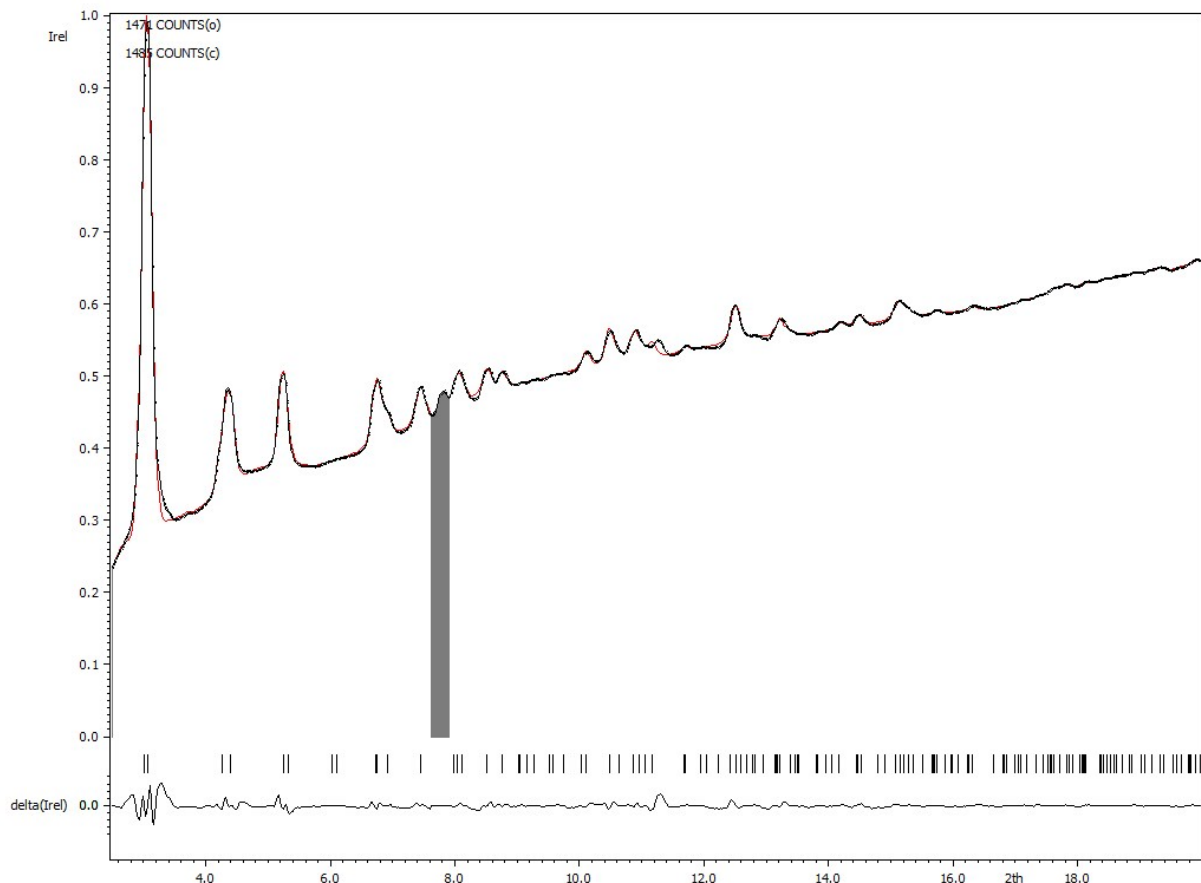


Figure S8. Structure-independent refinement of the unit-cell of the diffraction pattern obtained for the MIL-125(Ti), space group $I4/mmm$: $a=18.738(3)$ Å, $c=18.202(4)$ Å, $V=6224.1(3)$ Å 3 (R_p : 0.43, R_{wp} : 0.57) at atmospheric pressure after releasing the pressure (last step of the experiment).

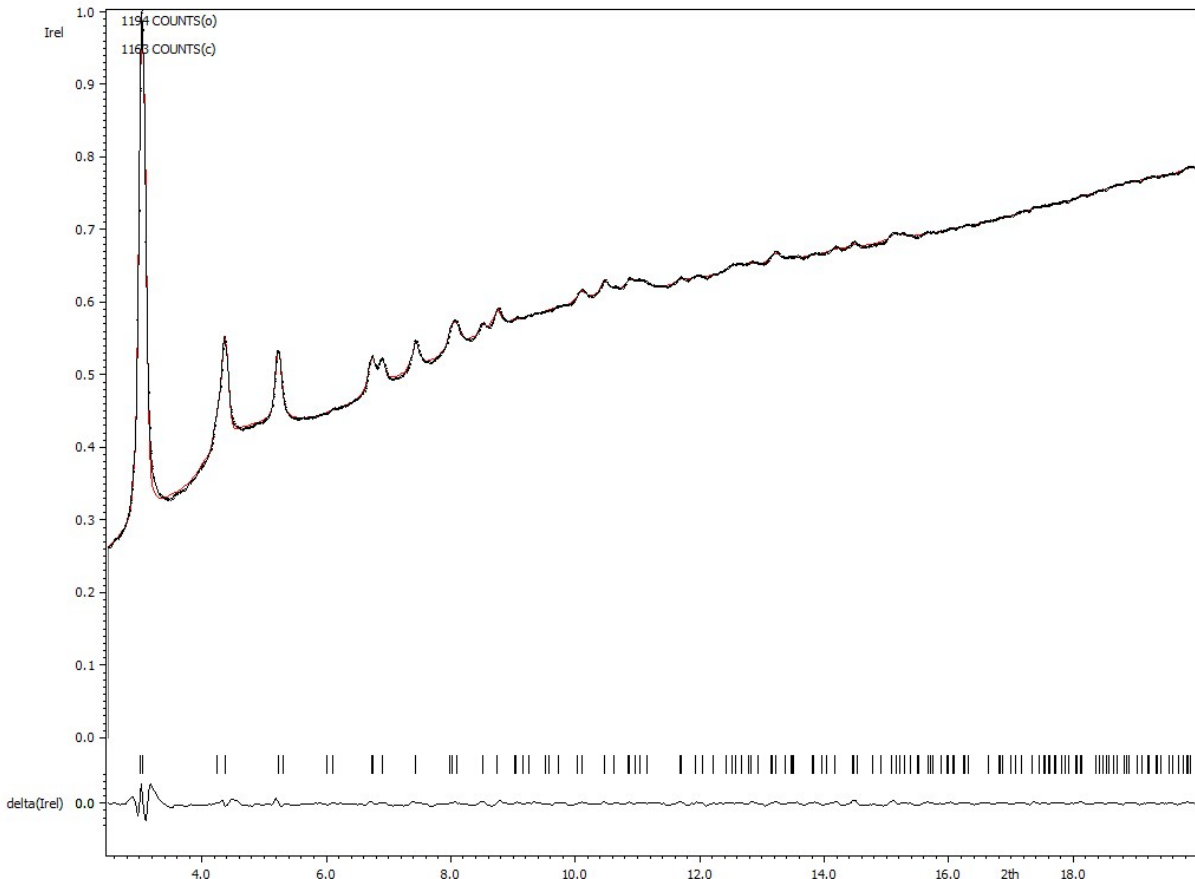


Figure S9. Structure-independent refinement of the unit-cell of the diffraction pattern obtained for the MIL-125(Ti)-NH₂, space group I4/mmm: $a=18.712(4)$ Å, $c=18.203(4)$ Å, $V=6373.4(4)$ Å³ (R_p : 0.28, R_{wp} : 0.34). at atmospheric pressure after releasing the pressure (last step of the experiment).

2. Crystal size and crystallinity determination

In the mean-time, one observes for both solids a significant broadening of the peaks for pressures above 0.5-1.0 GPa. This observation suggests that these materials undergo a loss of crystallinity in this range of pressures.

The Scherrer equation was employed to estimate the size of the crystal size $D = \frac{K\lambda}{\Delta \cos \theta}$ where K dimensionless shape factor was taken equal to 0.9, Wavelength $\lambda=0.69412$ Å, θ the Bragg angle of the most intense diffraction peak (111) one corresponding to $2\theta \sim 3.3^\circ$ and Δ the Full Width at Half Maximum (FWHM) of this peak.

The crystallinity labeled as C was then estimated using $C = \frac{D_0}{D_P} = \frac{\Delta_P \cos \theta_P}{\Delta_0 \cos \theta_0}$ where the symbols '0' and 'P' correspond to the situation under atmospheric pressure (initial stage) and under a given pressure applied respectively.

3. Bulk modulus determination

The bulk modulus K of the solids have been estimated from the unit cell volume by using the following equation : $K = V_0 \left(\frac{\partial P}{\partial V} \right)$ where V_0 is the volume of the initial phase. The bulk modulus is then related to the slope of the volume vs. pressure curve.

Table S2. Bulk modulus values obtained for the UiO-66(Zr) and MIL-125(Ti) and their amino-functionalized versions.

	UiO-66(Zr)	UiO-66(Zr)_{NH₂}	MIL-125(Ti)	MIL-125(Ti)_{NH₂}
Bulk modulus K (GPa)	17(1.5)	25(2)	10(2)	12(1.5)

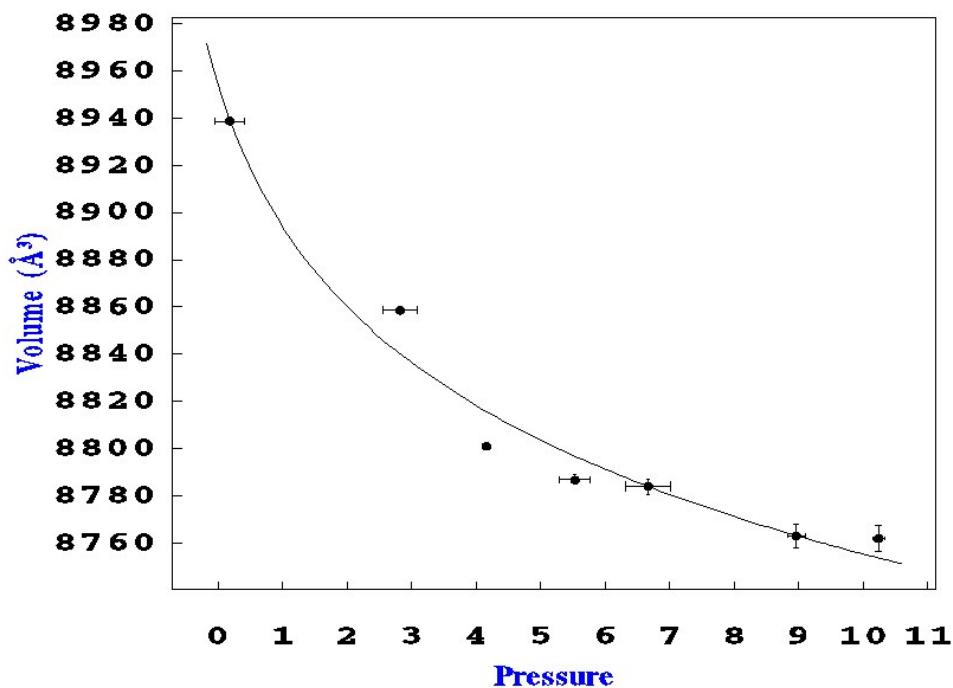


Figure S10. Evolution of the unit cell volume as a function of the applied pressure (in kbar) for the UiO-66(Zr).

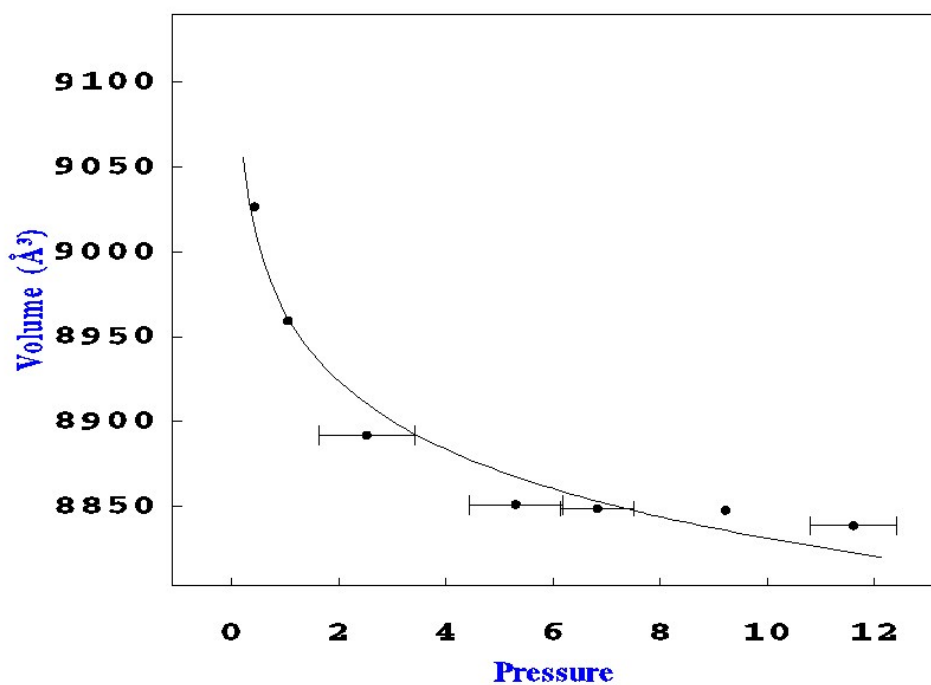


Figure S11. Evolution of the unit cell volume as a function of the applied pressure (in kbar) for the $\text{UiO-66}(\text{Zr})\text{-NH}_2$.

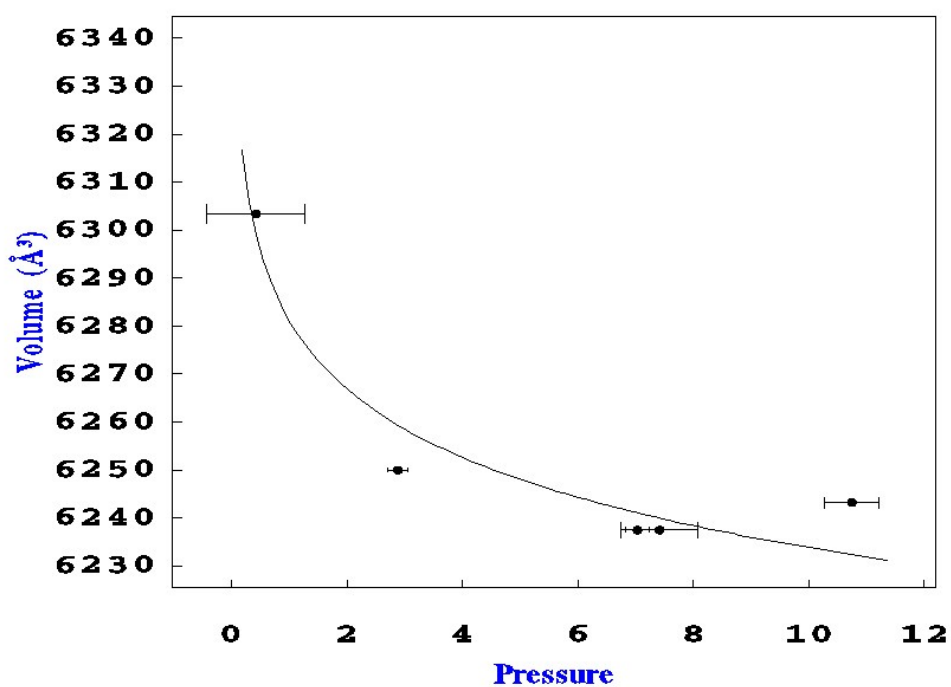


Figure S12. Evolution of the unit cell volume as a function of the applied pressure (in kbar) for the MIL-125(Ti).

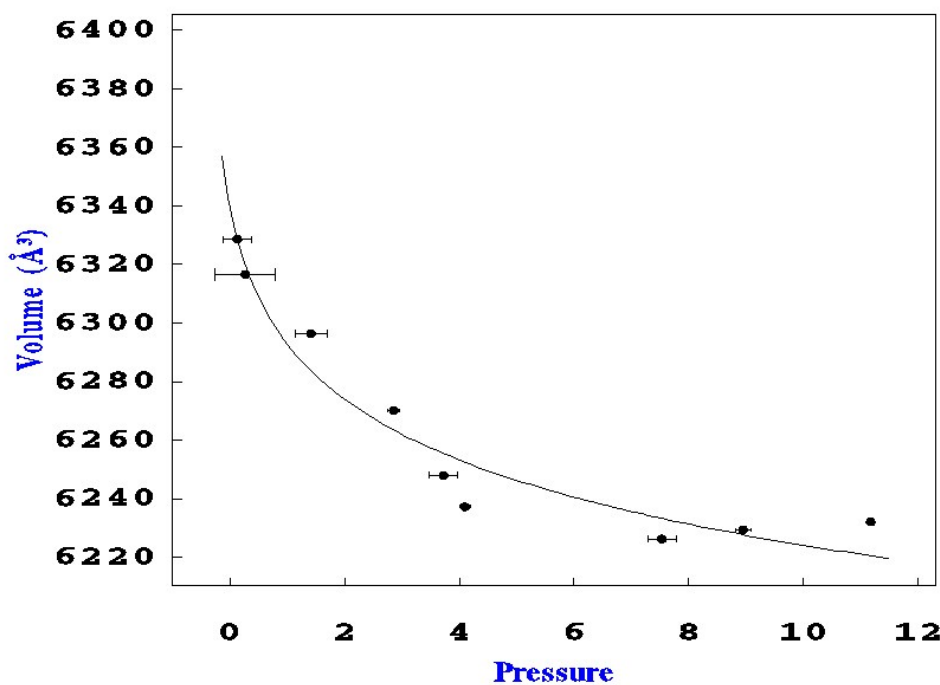


Figure S13. Evolution of the unit cell volume as a function of the applied pressure (in kbar) for the MIL-125(Ti)₂NH₂.

Table S3. Bulk modulus values obtained for different Metal Organic Frameworks materials.

Materials	Bulk modulus (GPa)	Method	Reference
MOF-5	~17.0	DFT	[8]
	~18.2	DFT	[9]
	~18.5	DFT	[10]
	~17.0	DFT	[11]
	~20.0	Forcefield based	[12]
	~14.4	Forcefield based	[13]
	~15.34	DFT	[14]

	~16.66	Forcefield based	[15]
IRMOF-8	~11.28	Forcefield based	[15]
IRMOF-14	~10.05	Forcefield based	[15]
MOF-C22	~6.88	Forcefield based	[15]
MOF-C30	~4.11	Forcefield based	[15]
MOF-177	~10.10	DFT	[14]
DUT-6	~10.73	DFT	[14]
MOF-14 (interpenetrated)	~14.8	DFT	[16]
MOF-14 (single net)	~5.5	DFT	[16]
DUT-34	~9.1	DFT	[16]
DUT-23	~13.2	DFT	[16]
HKUST-1(Cu-BTC)	~30.7	Experiment (No fluid)	[17]
	~29.5	Experiment (Fluorinert)	[17]
	~25	DFT	[18]
	~35.2	Forcefield based	[19]
	~24.53	DFT	[20]
UIO-66	~41.01	DFT	[20]
Hf-UiO-66	~39.49	DFT	[20]
Ti-UiO-66	~42.07	DFT	[20]
UiO-67	~17.15	DFT	[20]
UiO-68	~14.40	DFT	[20]
ZIF-4-1	~15.2	Experiment (Daphne Oil 7474)	[21]
ZIF-4	~7.78	Experiment (Daphne Oil 7474)	[21]
Zn(Im) ₂	~14	Experiment (Anhydrous 2-propanol)	[22]
LiB(Im) ₄	~16.6	Experiment (Anhydrous 2-propanol)	[23]

ZIF-8	~6.5	Experiment (Fluorinert)	[24]
	~9.23	DFT	[25]
	~7.75	Experiment (No fluid)	[25]
NH ₂ -MIL-53(Ind)	~10.09	Experiment (Mineral oil)	[26]
MIL-53(Cr)(Large-pore form)	~1.8	Forcefield based	[27]

4. Molecular Dynamics details

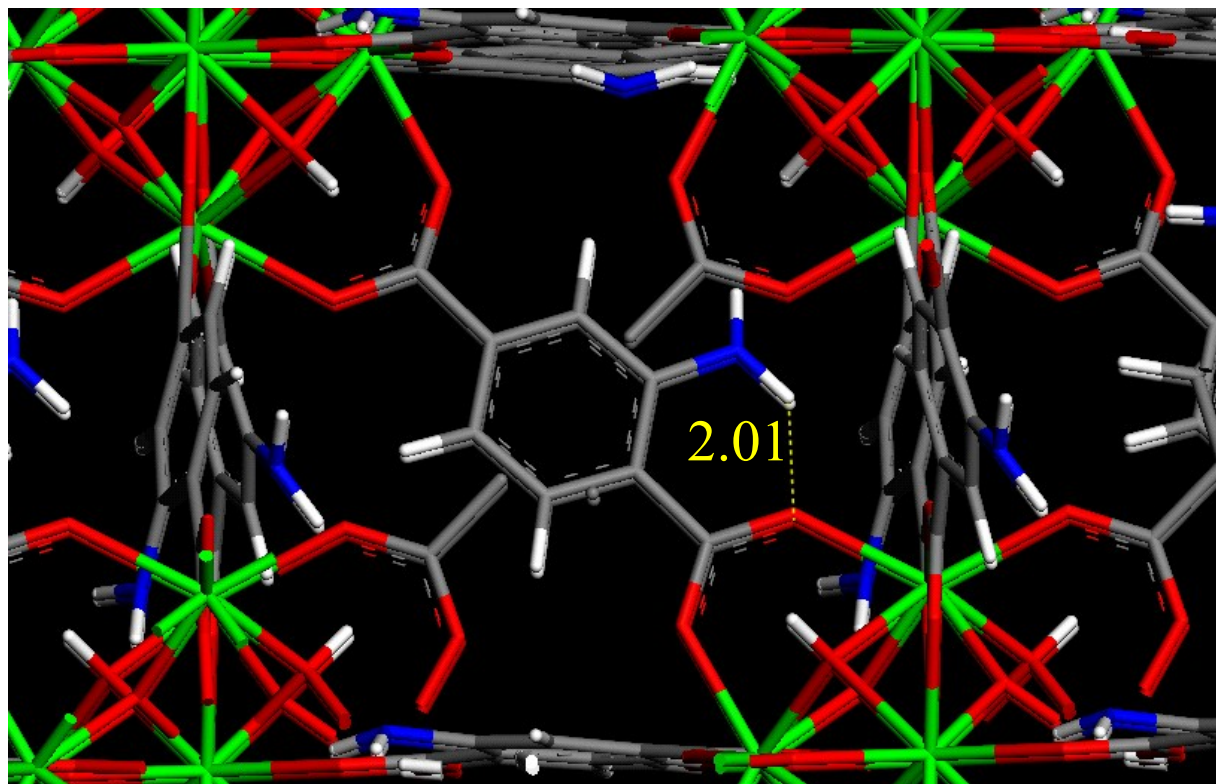


Figure S14. Illustration of the intra-framework interactions between the $-NH_2$ group and the inorganic evidenced by previous DFT calculations. The corresponding distances are reported in Å. The Zr, O, C, H and N atoms are represented in green, red, gray, white and blue, respectively.

References

- [1] J. Hafizovic Cavka, S. Jakobsen, U. Olsbye, N. Guillou, C. Lamberti, S. Bordiga and K. P. Lillerud, *J. Am. Chem. Soc.*, 2008, **130**, 13850.

- [2] M. Kandiah, M. H. Nilsen, S. Usseglio, S. Jakobsen, U. Olsbye, M. Tilset, C. Larabi, E. A. Quadrelli, F. Bonino and K. P. Lillerud, *Chem. Mater.*, 2010, **22**, 6632.
- [3] G. C. Shearer, S. Chavan, J. Ethiraj, J. G. Vitillo, S. Svelle, U. Olsbye, C. Lamberti, S. Bordiga and K. P. Lillerud, *Chem. Mater.*, 2014, **26**, 4068–4071.
- [4] H. K. Mao, J. Xu, P. M. Bell, *J. Geophys. Res.*, 1986, **91**, 4673.
- [5] A. P. Hammersley, S. O. Svensson, M. Hanfland, A. N. Fitch, D. Häusermann, *High Press. Res.*, 1996, **14**, 235.
- [6] A. Boultif, D. Louer, *J. Appl. Crystallogr.*, 1991, **24**, 987.
- [7] V. Petricek, M. Dusek, L. Palatinus, *Z. Kristallogr.*, 2014, **229**, 345.
- [8] M. Mattesini, J. M. Soler, F. Ynduráin, *Phys. Rev. B*, 2006, **73**, 094111.
- [9] W. Zhou, T. Yildirim, *Phys. Rev. B*, 2006, **74**, 180301.
- [10] A. Samanta, T. Furuta, J. Li, *J. Chem. Phys.*, 2006, **125**, 084714.
- [11] D. Bahr, J. Reid, W. Mook, C. Bauer, R. Stumpf, A. Skulan, N. Moody, B. Simmons, M.; Shindel, M. Allendorf, *Phys. Rev. B*, 2007, **76**, 184106.
- [12] J. A. Greathouse, M. D. Allendorf, *J. Phys. Chem. C*, 2008, **112**, 5795.
- [13] M. Tafipolsky, R. Schmid, *J. Phys. Chem. B*, 2009, **113**, 1341.
- [14] B. Lukose, B. Supronowicz, P. St. Petkov, J. Frenzel, A. B. Kuc, G. Seifert, G. N. Vayssilov, T. Heine, *Phys. Status Solidi B*, 2012, **249**, 335.
- [15] S. S. Han, W. A. Goddard, *J. Phys. Chem. C*, 2007, **111**, 15185.
- [16] N. Klein, I. Senkovska, I. A. Baburin, R. Gruenker, U. Stoeck, M. Schlichtenmayer, B. Streppel, U. Mueller, S. Leoni, M. Hirscher, S. Kaskel, *Chem. Eur. J.*, 2011, **17**, 13007.
- [17] K. W. Chapman, G. J. Halder, P. J. Chupas, *J. Am. Chem. Soc.*, 2008, **130**, 10524.
- [18] M. Tafipolsky, S. Amirjalayer, R. Schmid, *J. Phys. Chem. C*, 2010, **114**, 14402.
- [19] L. Zhao L, Q. Yang, Q. Ma, C. Zhong, J. Mi, D. Liu, *J Mol Model.*, 2011, **17**, 227.
- [20] H. Wu, T. Yildirim, W. Zhou, *J. Phys. Chem. Lett.*, 2013, **4**, 925.
- [21] T. D. Bennett, P. Simoncic, S. A. Moggach, F. Gozzo, P. Macchi, D. A. Keen, J.-C. Tan and A. K. Cheetham, *Chem. Commun.*, 2011, **47**, 7983.
- [22] E. C. Spencer, R. J. Angel, N. L. Ross, B. E. Hanson, J. A. K. Howard, *J. Am. Chem. Soc.*, 2009, **131**, 4022.

- [23] T. D. Bennett, J. C. Tan, S. A. Moggach, R. Galvelis, C. Mellot-Draznieks, B. A. Reisner, A. Thirumurugan, D. R. Allan, A. K. Cheetham, *Chem. Eur. J.*, 2010, **16**, 10684.
- [24] K. W. Chapman, G. J. Halder, P. J. Chupas, , *J. Am. Chem. Soc.*, 2009, **131**, 17546.
- [25] J. C. Tan, B. Civalleri, C. C. Lin, L. Valenzano, R. Galvelis, P. F. Chen, T. D. Bennett, C. Mellot-Draznieks, C. M. Zicovich-Wilson, A. K. Cheetham, *Phys. Rev. Lett.*, 2012, **108**, 095502.
- [26] P. Serra-Crespo, E. Stavitski, F. Kapteijn, J. Gascon, *RSC Advances*, 2012, **2**, 5051.
- [27] Q. Ma, Q. Yang, A. Ghoufi, G. Ferey, C. Zhong, G. Maurin, *Dalton Trans.*, 2012, **41**, 3915.